

# Carbide Formation and Dissolution in Biomedical Co-Cr-Mo Alloys with Different Carbon Contents during Solution Treatment

SHINGO MINETA, SHIGENOBU NAMBA, TAKASHI YONEDA, KYOSUKE UEDA, and TAKAYUKI NARUSHIMA

The microstructures of as-cast and heat-treated biomedical Co-Cr-Mo (ASTM F75) alloys with four different carbon contents were investigated. The as-cast alloys were solution treated at 1473 to 1548 K for 0 to 43.2 ks. The precipitates in the matrix were electrolytically extracted from the as-cast and heat-treated alloys. An  $M_{23}C_6$  type carbide and an intermetallic  $\sigma$  phase (Co(Cr,Mo)) were detected as precipitates in the as-cast Co-28Cr-6Mo-0.12C alloy; an  $M_{23}C_6$  type carbide, a  $\sigma$  phase, an  $\eta$  phase ( $M_6C$ - $M_{12}C$  type carbide), and a  $\pi$  phase ( $M_2T_3X$  type carbide with a  $\beta$ -manganese structure) were detected in the as-cast Co-28Cr-6Mo-0.15C alloy; and an  $M_{23}C_6$  type carbide and an  $\eta$  phase were detected in the as-cast Co-28Cr-6Mo-0.25C and Co-28Cr-6Mo-0.35C alloys. After solution treatment, complete precipitate dissolution occurred in all four alloys. Under incomplete precipitate dissolution conditions, the phase and shape of precipitates depended on the heat-treatment conditions and the carbon content in the alloys. The  $\pi$  phase was detected in the alloys with carbon contents of 0.15, 0.25, and 0.35 mass pct after heat treatment at high temperature such as 1548 K for a short holding time of less than 1.8 ks. The presence of the  $\pi$  phase in the Co-Cr-Mo alloys has been revealed in this study for the first time.

DOI: 10.1007/s11661-010-0227-1

© The Minerals, Metals & Materials Society and ASM International 2010

## I. INTRODUCTION

THE Co-Cr-Mo alloys are currently applied as primary materials for orthopedic implants, in addition to stainless steels and titanium and its alloys, owing to their advantageous properties such as excellent mechanical properties, high corrosion resistance, and high wear resistance.<sup>[1-4]</sup> Standard cast Co-Cr-Mo alloys, registered as ASTM F75, have been used to manufacture biomedical devices such as artificial joints and denture bases because of their high wear resistance, which can be attributed to precipitation strengthening by carbides formed in the matrix.<sup>[5-7]</sup>

Cast Co-Cr-Mo alloys are subjected to heat treatment in order to remove casting defects and improve their mechanical properties. Therefore, the behavior of carbides formed in Co-Cr-Mo alloys during heat treatment has been investigated in some studies.<sup>[8-18]</sup> Several studies have focused on investigating the dissolution behavior of carbides during solution treatment.<sup>[8-16]</sup> Although the precipitation or dissolution behavior of carbides is essential knowledge to establish an effective and low-cost manufacturing process for Co-Cr-Mo

alloys, a systematic explanation of the behavior of carbides during solution treatment has not been reported thus far.

Therefore, the objective of this study is to investigate the microstructural changes that take place during the solution treatment in Co-Cr-Mo-C alloys with various carbon contents. On the basis of the observations and analyses, the phase, shape, and dissolution behavior of precipitates in the Co-Cr-Mo-C alloys are discussed.

## II. EXPERIMENTAL PROCEDURE

### A. Specimens

Cast Co-Cr-Mo alloys with various carbon contents were investigated in this study; their chemical composition was Co-28Cr-6Mo- $x$ C ( $x = 0.12, 0.15, 0.25,$  and  $0.35$  mass pct). Table I lists the chemical compositions of these alloys. Hereafter, these alloys with carbon contents of 0.12, 0.15, 0.25, and 0.35 mass pct are referred to as C12, C15, C25, and C35, respectively. Ingots of these alloys were induction melted under Ar atmosphere and cast in a copper mold. The size of the fabricated ingots was 33 mm in diameter and 100 mm in height. The ingots were cut into disks having a diameter and thickness of 33 and 5 mm, respectively. Plate specimens were then prepared by dividing each disk into six equal parts.

### B. Solution Treatment

The plate specimens were heat treated at 1473 to 1548 K for 0 to 43.2 ks in Ar atmosphere with a gas flow rate of  $1.7 \times 10^{-6} \text{ m}^3 \cdot \text{s}^{-1}$ ; they were then water

SHINGO MINETA, Graduate Student, KYOSUKE UEDA, Assistant Professor, and TAKAYUKI NARUSHIMA, Professor, are with the Department of Materials Processing, Tohoku University, Sendai, 980-8579, Japan. Contact e-mail: a9td5609@s.tohoku.ac.jp SHIGENOBU NAMBA, Senior Research Metallurgist is with the Materials Research Laboratory, Kobe Steel, Ltd., Kobe, 651-2271, Japan. TAKASHI YONEDA, President, is with the Yoneda Advanced Casting Co., Ltd., Takaoka, 933-0951, Japan.

Manuscript submitted November 4, 2009.

Article published online May 7, 2010

**Table I. Compositions of Co-Cr-Mo-C Alloys Used in Solution Treatment (Mass Percent)**

Alloy	Co	Cr	Mo	C	Si	Mn	P	S	N
C12	bal	28.8	6.30	0.12	0.12	0.056	0.011	0.004	—
C15	bal	27.5	6.04	0.16	0.09	0.039	<0.001	<0.001	0.004
C25	bal	27.7	6.11	0.26	0.09	0.039	<0.001	<0.001	0.005
C35	bal	27.4	6.03	0.35	0.09	0.039	<0.001	<0.001	0.004

quenched. A specimen was inserted into the electric resistance tube furnace maintained at the specified temperature in Ar atmosphere to initiate heat treatment. The specimen temperature reached the specified value 0.5 ks after being placed in the hot zone of the tube furnace. A holding time of 0 ks implies that the specimens were water quenched immediately after the specimen temperature reached a specified value.

For microstructural observations, the as-cast and heat-treated plate specimens were wet polished with emery papers up to a grit size of 1500 and buff polished with a diamond paste having a grain size of 0.1  $\mu\text{m}$ . The specimens were electrolytically etched at 6 V in 10 pct  $\text{H}_2\text{SO}_4$ -methanol solution,<sup>[3]</sup> and their microstructures were observed using an optical microscope (OM, Olympus Co., BX60M, Tokyo, Japan), a scanning electron microscope (SEM, PHILIPS,\* XL30FEG), an

\*PHILIPS is a trademark of FEI Company, Hillsboro, OR.

energy dispersive X-ray spectrometer (EDX, EDAX, DX-4 CDU NEW XL-30, AMETEK Inc., Mahwah, NJ), and a transmission electron microscope (TEM, JEOL,\*\* JEM-2100). In the TEM analysis, the camera

\*\*JEOL is a trademark of Japan Electron Optics Ltd., Tokyo.

length and the accelerating voltage are 850 mm and 200 kV, respectively. The amounts of precipitates formed in the matrix were evaluated as the ratio of area occupied by precipitates to the total area in the OM images of the microstructure.

Precipitates formed in the as-cast and heat-treated specimens were electrolytically extracted in 10 pct  $\text{H}_2\text{SO}_4$  aqueous solution at 2 V. The phase of the extracted precipitates was identified using an X-ray diffractometer (XRD, Bruker AXS, D8 ADVANCE, Karlsruhe, Germany), and XRD patterns were obtained using  $\text{Cu } K_\alpha$  radiation.

### III. RESULTS

#### A. Microstructure of As-Cast Co-Cr-Mo-C Alloys

Figure 1 shows the microstructure of the as-cast C12, C15, C25, and C35 alloys. A dendrite matrix and interdendritic and grain boundary precipitates were observed in these alloys. The amount of precipitates formed in the matrix increased with the carbon content in the alloys. Figure 2 shows the XRD patterns of the

precipitates that were electrolytically extracted from the as-cast C12, C15, C25, and C35 alloys. The types of precipitates formed in the as-cast alloys depended on the carbon content. The precipitates observed in the matrix of the as-cast C12 alloy, a low-carbon-content alloy, were an  $\text{M}_{23}\text{C}_6$  type carbide and an intermetallic  $\sigma$  phase ( $\text{Co}(\text{Cr},\text{Mo})$ ).<sup>[4]</sup> In the case of as-cast C25 and C35 alloys, both of which are high-carbon-content alloys, several peaks assigned to the  $\eta$  phase ( $\text{M}_6\text{C}$ - $\text{M}_{12}\text{C}$  type carbide) were detected. The  $\text{M}_6\text{C}$  type and  $\text{M}_{12}\text{C}$  type carbides had similar crystallographic structures.<sup>[19]</sup> Thus, both these carbides are classified into the  $\eta$  phase.<sup>[20-22]</sup> Therefore, the precipitates formed in the as-cast C25 and C35 alloys are concluded to be the  $\text{M}_{23}\text{C}_6$  type carbide and the  $\eta$  phase. In the case of the as-cast C15 alloy, the XRD pattern was complicated and revealed the presence of another phase in addition to the  $\text{M}_{23}\text{C}_6$  type carbide,  $\sigma$  phase, and  $\eta$  phase. The XRD reflections of this phase were in good agreement with the pattern of  $(\text{Cr},\text{Mo})_{12}(\text{Fe},\text{Ni})_{8-x}\text{N}_{4-z}$  type nitride,<sup>[23]</sup> which was detected as a precipitate after aging of the Fe-25Cr-28Ni-2Mo-0.31N alloy.<sup>[24]</sup> This nitride phase was referred to as the  $\pi$  phase; this phase exhibits a  $\beta$ -manganese structure and its chemical composition can be represented by  $\text{M}_2\text{T}_3\text{X}$  (X: carbon or nitrogen).<sup>[24]</sup> With regard to the carbides,  $\text{Al}_2\text{Mo}_3\text{C}$  fabricated by the sintering method was reported to be an  $\text{M}_2\text{T}_3\text{X}$  type carbide with a  $\beta$ -manganese structure, although it was not referred to as a  $\pi$  phase.<sup>[25]</sup> In this article, we refer to the phase in the as-cast C15 alloy as a  $\pi$  phase ( $\text{M}_2\text{T}_3\text{X}$  type carbide with a  $\beta$ -manganese structure). The lattice constant of the  $\pi$  phase formed in as-cast C15 alloys was calculated using the XRD pattern, assuming the  $\beta$ -manganese structure; the value of the lattice constant was 0.638 nm. This lattice constant agreed well with the value of 0.636 nm obtained in the case of  $(\text{Cr},\text{Mo})_{12}(\text{Fe},\text{Ni})_{8-x}\text{N}_{4-z}$ .<sup>[23]</sup> The formation of the  $\pi$  phase has not been reported in biomedical Co-Cr-Mo-C alloys thus far.

#### B. Microstructural Change in Co-Cr-Mo-C Alloys during Solution Treatment

In this study, complete precipitate dissolution could be achieved in all 4 alloys. However, the solution treatment conditions for complete precipitate dissolution depended on the carbon content. Figures 3 and 4 show the microstructural changes in C12 and C35 alloys heat treated at 1473 K, respectively. In the C12 alloy, complete precipitate dissolution was observed after 1.8 ks. On the contrary, the precipitates formed in the C35 alloy remained even after 43.2 ks. Solution treatment at 1523 or 1548 K was required to completely

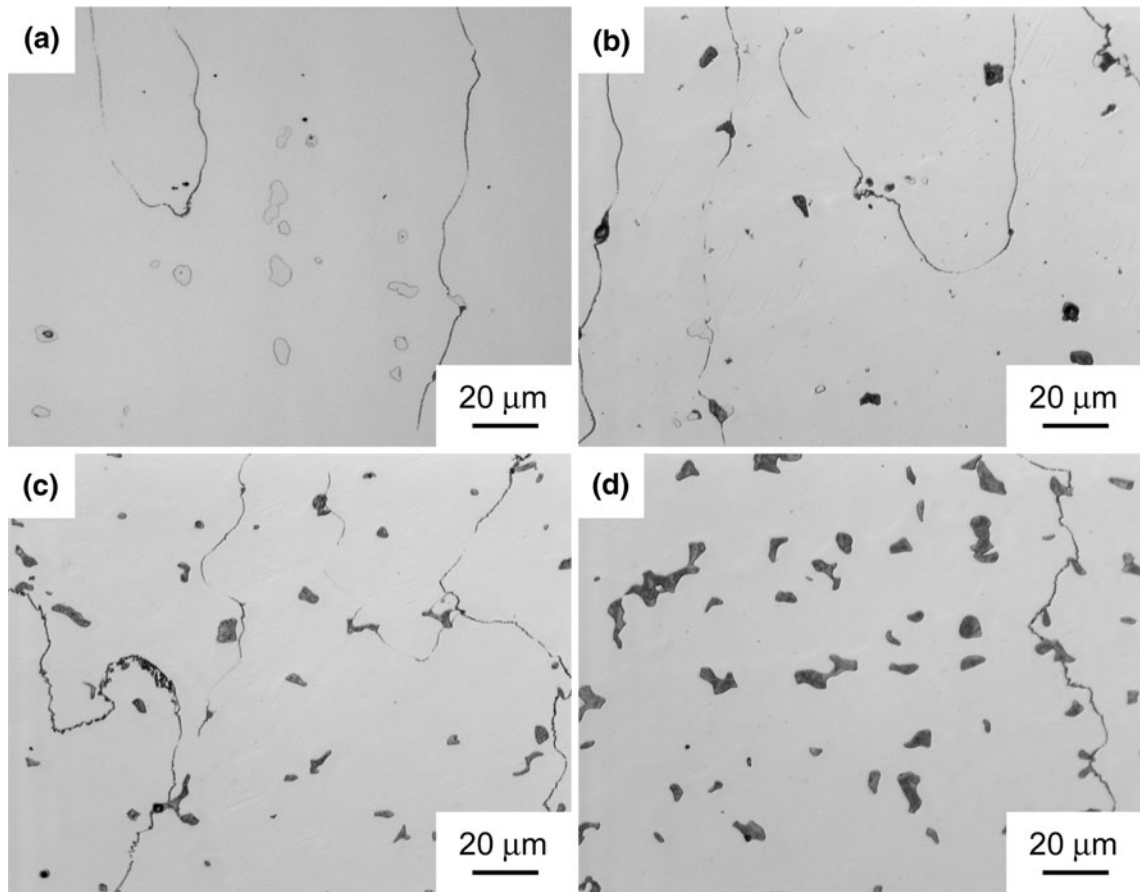


Fig. 1—Microstructure of as-cast (a) C12, (b) C15, (c) C25, and (d) C35 alloys.

dissolve precipitates in the C35 alloy. Figures 5 and 6 show the variation in the microstructure of the C35 alloy with holding time at 1523 and 1548 K, respectively. The amount of precipitates decreased with an increase in the holding time, and the precipitates were completely dissolved after 43.2 and 21.6 ks at 1523 and 1548 K, respectively. The morphology of precipitates formed in the matrix during solution treatment depended on the solution treatment temperature. The morphology of precipitates is mentioned in Section D. Solution treatment conditions for complete precipitate dissolution are summarized in Figure 7. In the temperature range between 1473 and 1548 K, the holding time required for complete carbide dissolution increased with an increase in carbon content and a decrease in solution treatment temperature.

### C. Types of Precipitates in Heat-Treated Co-Cr-Mo-C Alloys

Under incomplete precipitate dissolution conditions, the types of the precipitates formed in the alloys depended on the carbon content and the heat-treatment condition. Figures 8 through 11 show the XRD patterns of the precipitates that were electrolytically extracted from the C12, C15, C25, and C35 alloys heat treated in the temperature range between 1473 and 1548 K for 0 ks, respectively. The observed precipitates in the C12

alloy were the  $M_{23}C_6$  type carbide and  $\sigma$  phase. In the C15 alloy, the  $M_{23}C_6$  type carbide was mainly observed at 1473 and 1498 K, but the  $\pi$  phase and  $M_{23}C_6$  type carbide were observed at 1523 and 1548 K. In the case of the C25 and C35 alloys, the  $M_{23}C_6$  type carbide was observed at 1473, 1498, and 1523 K, and the  $M_{23}C_6$  type carbide and  $\pi$  phase were observed at 1548 K.

Figure 12 shows the XRD pattern of the precipitates that were electrolytically extracted from the C35 alloy heat treated at 1548 K. The amount of  $\pi$  phase decreased with an increase in the holding time, and the  $\pi$  phase could not be observed after heat treatment at 1548 K for a holding time longer than 1.8 ks.

### D. Morphology of Precipitates in Heat-Treated Co-Cr-Mo-C Alloys

Under incomplete precipitate dissolution conditions, the morphology of the carbide changed depending on the heat-treatment temperature. In the C15 alloy heat treated at 1473 and 1498 K, and the C25 and C35 alloys heat treated at 1473, 1498, and 1523 K, the morphology of the  $M_{23}C_6$  type carbide was blocky-dense.<sup>[8]</sup> Typical blocky-dense  $M_{23}C_6$  type carbide is shown in Figure 13. At high temperatures such as 1548 K, however, the shape of precipitates formed in the alloys was starlike. The SEM images of the precipitates in the C35 alloy

heat treated at 1548 K for 0 ks are shown in Figure 14. Two types of starlike precipitates were observed in the C35 alloy heat treated for 0 ks. One was a starlike precipitate that had a stripe pattern; the other was a starlike-dense precipitate that did not have the stripe pattern. After 1.8 ks, only the starlike precipitate with the stripe pattern was detected. Figure 15 shows the TEM images of the starlike precipitate with the stripe pattern formed in the C35 alloy heat treated at 1548 K for 0 ks. Electron diffraction revealed that the starlike precipitate with the stripe pattern consisted of the  $M_{23}C_6$  type carbide and metallic  $\gamma$  phase

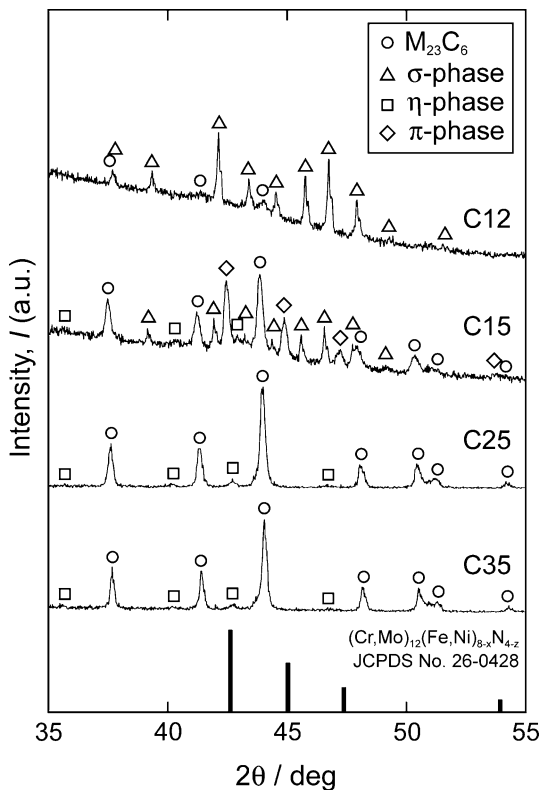


Fig. 2—XRD patterns of precipitates that were electrolytically extracted from as-cast C12, C15, C25, and C35 alloys.

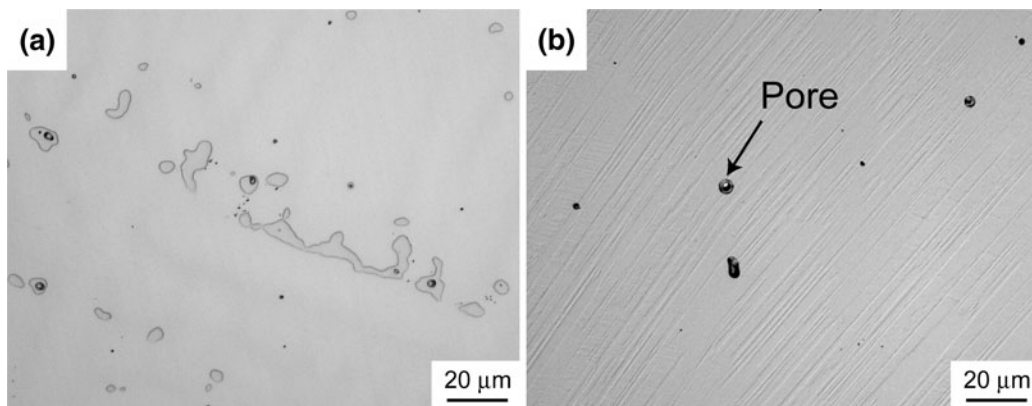


Fig. 3—Microstructure of the C12 alloy with holding times of (a) 0 and (b) 1.8 ks at 1473 K.

(face-centered-cubic matrix). The results of TEM analysis of the starlike precipitate with no stripe pattern observed in the C35 alloy heat treated at 1548 K for 0 ks are shown in Figure 16. It was found that the starlike-dense precipitate was the  $\pi$  phase. The composition ratios of major metallic elements in the  $M_{23}C_6$  type carbide and the  $\pi$  phase were analyzed using SEM-EDX. The composition ratios of Co, Cr, and Mo in the  $M_{23}C_6$  type carbide and the  $\pi$  phase were Co:Cr:Mo = 27:61:12 and 38:49:13 in at. pct, respectively. The ideal composition of the  $\pi$  phase was expressed as  $T_{12}M_8X_4$  ( $=M_2T_3X$ ), where M and T are metallic elements and X is carbon or nitrogen.<sup>[24]</sup> In the Fe-25Cr-28Ni-2Mo-0.31N alloys, Kikuchi *et al.* reported that the  $\pi$  phase has been verified to be actually a nitride with a chemical formula of  $(Cr, Mo)_{12+x}(Fe, Ni)_{8-x}N_{4-y}$ .<sup>[24]</sup> Therefore, the ideal chemical formula of the  $\pi$  phase would be  $(Cr, Mo)_{12}(Fe, Ni)_8N_4$ , *i.e.*, M = Fe and Ni and T = Cr and Mo. Therefore, in the case of the Co-Cr-Mo-C system, it is ideally expected that M will be occupied by Co, and T will be occupied by Cr and Mo. The value of  $(Cr + Mo)/Co$  in the  $\pi$  phase of C35 alloys heat treated at 1548 K for 0 ks was calculated to be 1.62 at. pct. This value was comparable to the ideal value of 1.5.

#### IV. DISCUSSION

The types of precipitates detected in the C12, C15, C25, and C35 alloys in as-cast conditions and after heat treatment are summarized in Figure 17. The types of precipitates observed in the as-cast alloys depended on the carbon content. The  $\sigma$  phase decreased and the amount of the carbides increased with an increase in the carbon content. Ramírez *et al.* reported that the  $\sigma$  phase reacted with the solute carbon to form  $M_{23}C_6$  type and  $M_{12}C$  type carbides during the solidification of Co-Cr-Mo-C alloys.<sup>[18]</sup> The  $M_{12}C$  type carbide was reported to transform into the  $M_{23}C_6$  type carbide during the cooling of the as-cast Co-Cr-Mo-C alloys.<sup>[18]</sup> In this study, the XRD analysis of the precipitates that were electrolytically extracted from the as-cast alloys revealed the presence of the  $\eta$  phase in the C15, C25, and C35 alloys. This result is attributed to the cooling rate of

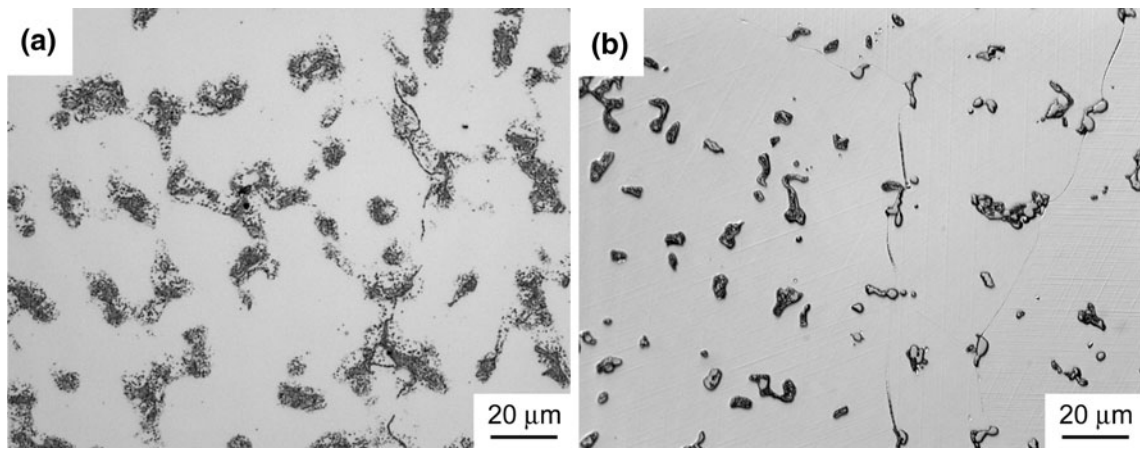


Fig. 4—Microstructure of the C35 alloy with holding times of (a) 0 and (b) 43.2 ks at 1473 K.

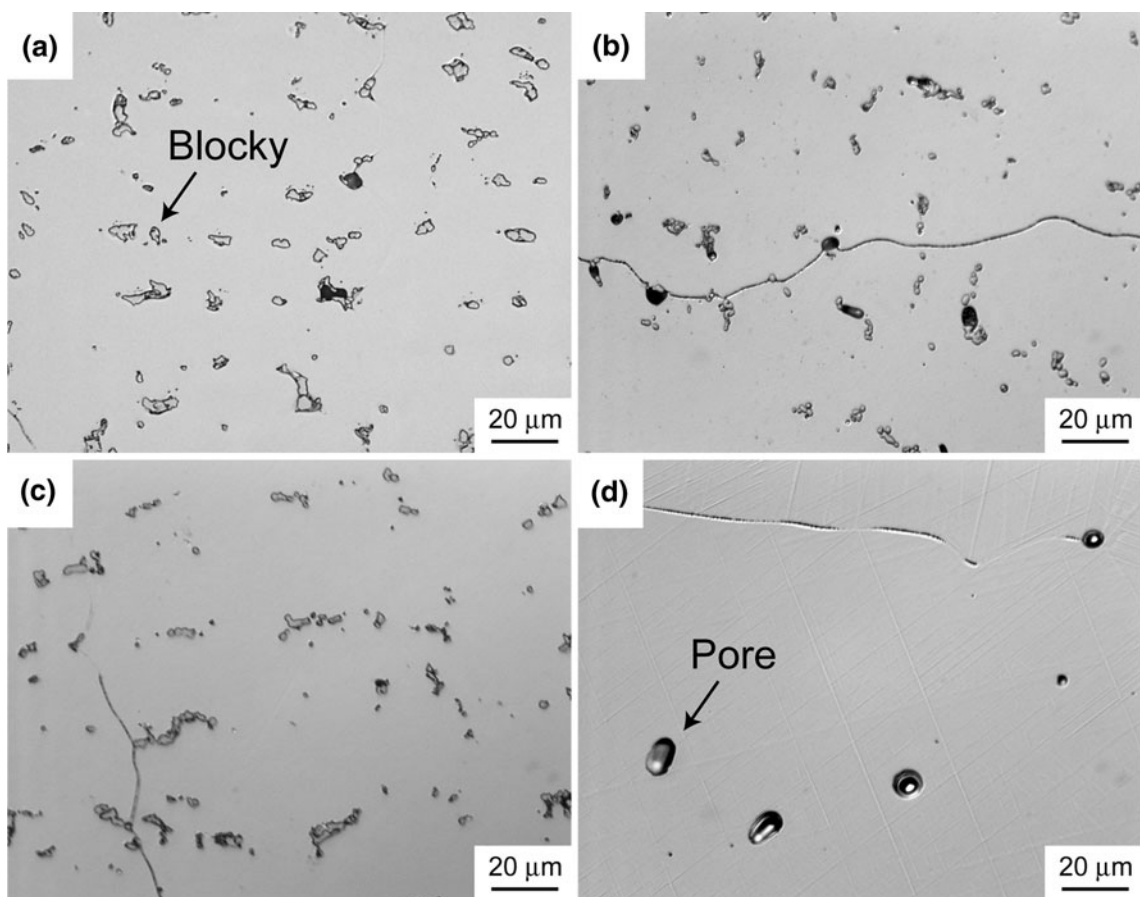


Fig. 5—Microstructure of the C35 alloy with holding times of (a) 0, (b) 1.8, (c) 7.2, and (d) 43.2 ks at 1523 K.

solidification for the cast employed in this study. In this study, a copper casting mold was used to prepare the Co-Cr-Mo-C alloy ingots. When the copper casting mold was used, the transformation of the  $\eta$  phase into the  $M_{23}C_6$  type carbide may not have been completed because of the high cooling rate, and the  $\eta$  phase remained in the as-cast Co-Cr-Mo alloys.

Complete precipitate dissolution could be achieved in all four Co-Cr-Mo-C alloys after solution treatment. For complete precipitate dissolution to occur during solution treatment, a high heat-treatment temperature and a long holding time were required with increasing carbon content in the Co-Cr-Mo alloys. The behavior of the carbides during solution treatment and the optimal

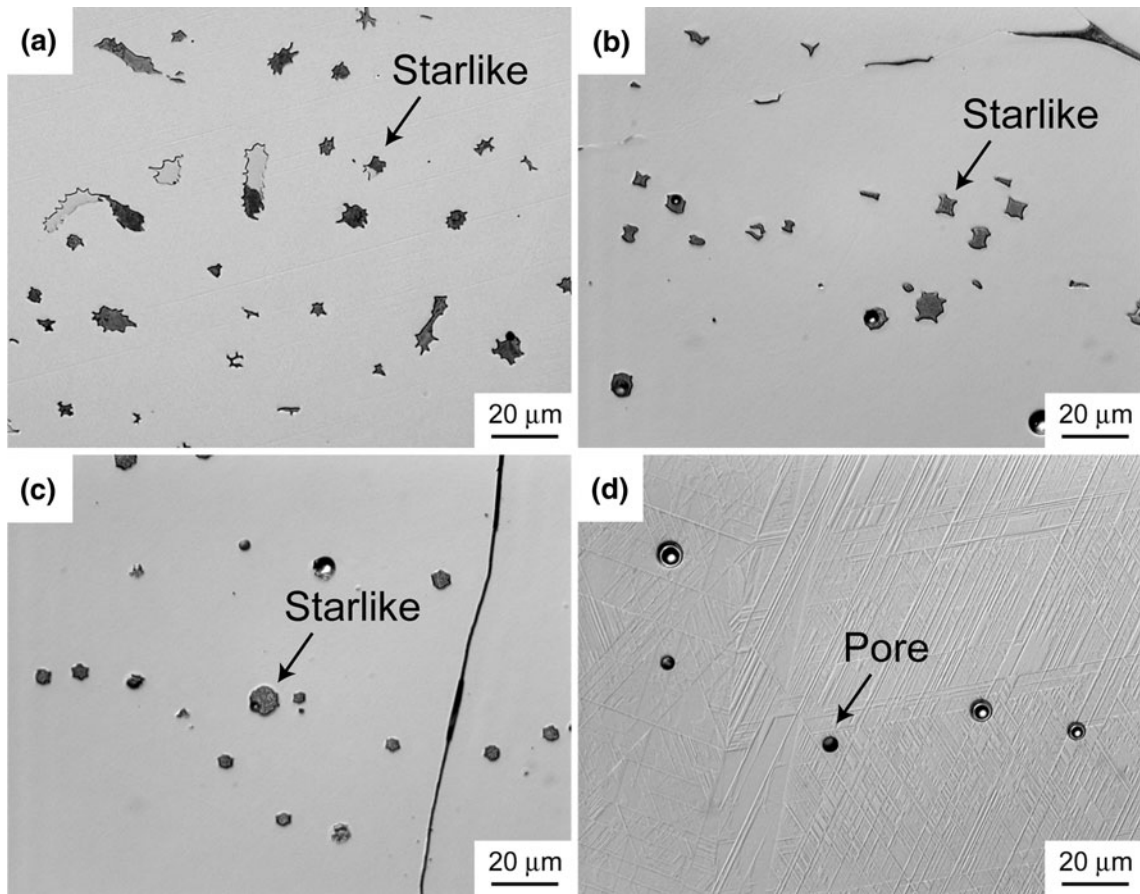


Fig. 6—Microstructure of the C35 alloy with holding times of (a) 0, (b) 1.8, (c) 7.2, and (d) 43.2 ks at 1548 K.

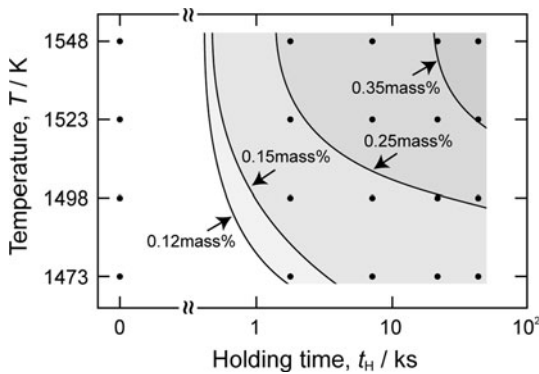


Fig. 7—Solution treatment conditions for the complete dissolution of precipitates in Co-Cr-Mo-C alloys.

solution treatment conditions have been investigated by other research groups.<sup>[8–16]</sup> Dobbs and Robertson observed incomplete carbide dissolution in a Co-28.9Cr-5.58Mo-0.24C alloy containing additional Si, Mn, Fe, Ni, Al, and Ti after heat treatment at 1513 K for 7.2 ks.<sup>[9]</sup> Herrera *et al.* reported incomplete precipitate dissolution in Co-27Cr-6Mo- $x$ C ( $x = 0.17, 0.23,$  and  $0.30$  mass pct) alloys that were heat treated at 1503 K for up to 14.4 ks.<sup>[10]</sup> In contrast, Clemow and Daniell reported complete precipitate dissolution in Co-Cr-Mo

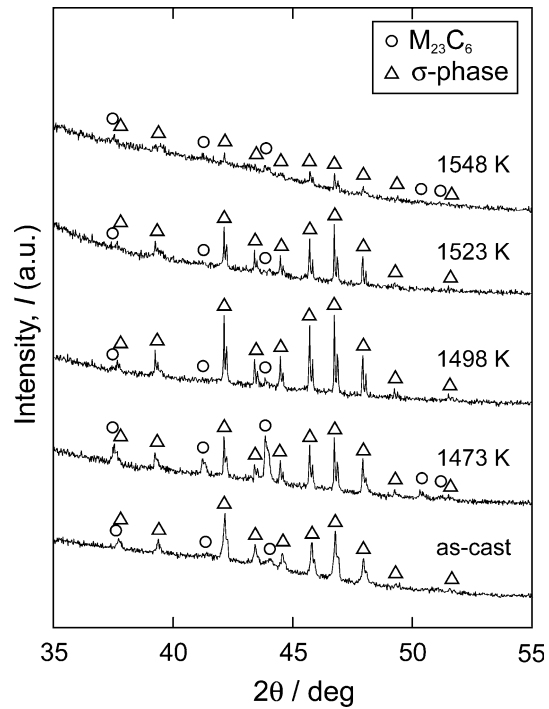


Fig. 8—XRD patterns of precipitates electrolytically extracted from the C12 alloy in as-cast condition and heat treated at various temperatures for 0 ks.

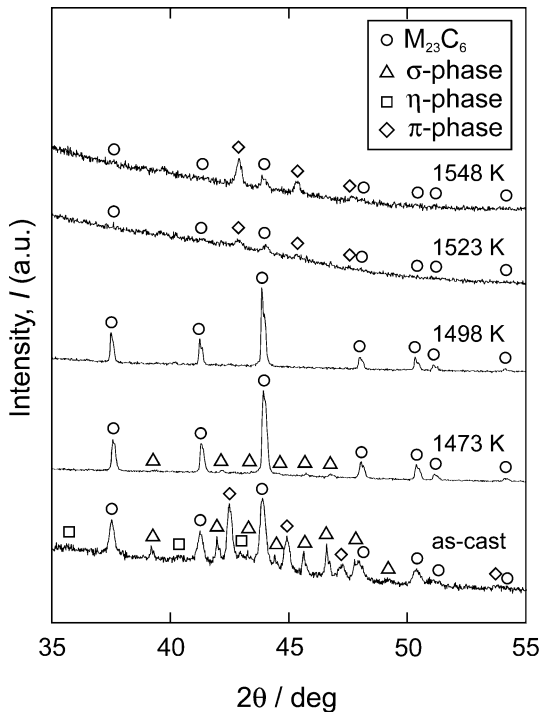


Fig. 9—XRD patterns of precipitates electrolytically extracted from the C15 alloy in as-cast condition and heat treated at various temperatures for 0 ks.

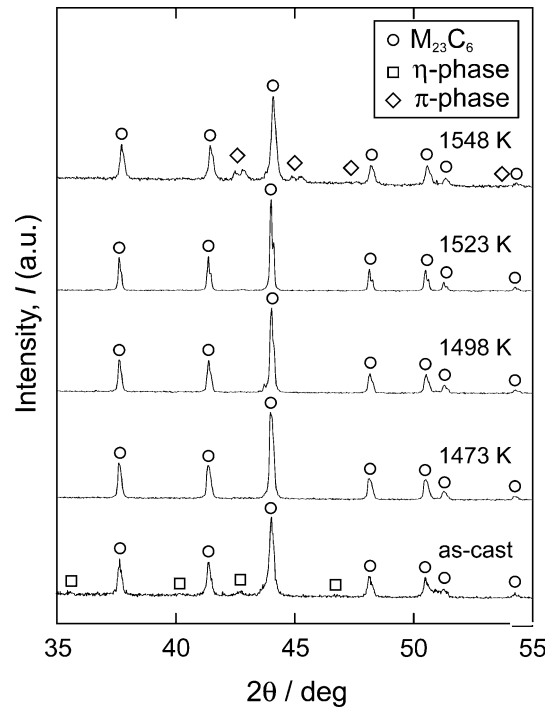


Fig. 11—XRD patterns of precipitates electrolytically extracted from the C35 alloy in as-cast condition and heat treated at various temperatures for 0 ks.

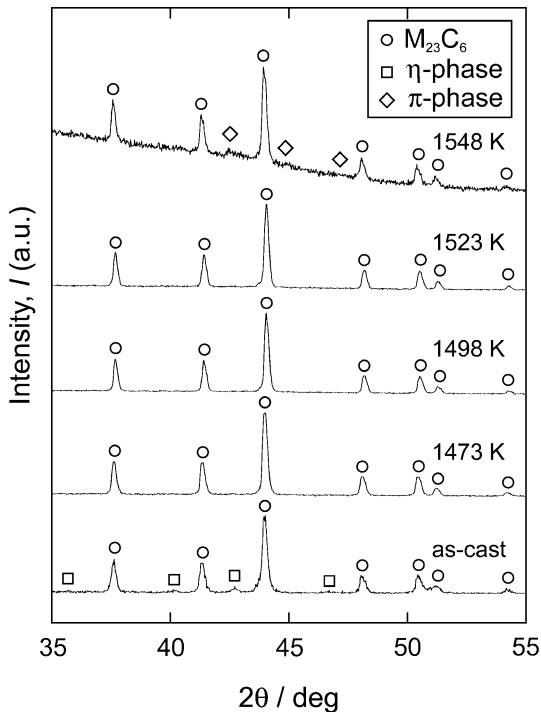


Fig. 10—XRD patterns of precipitates electrolytically extracted from the C25 alloy in as-cast condition and heat treated at various temperatures for 0 ks.

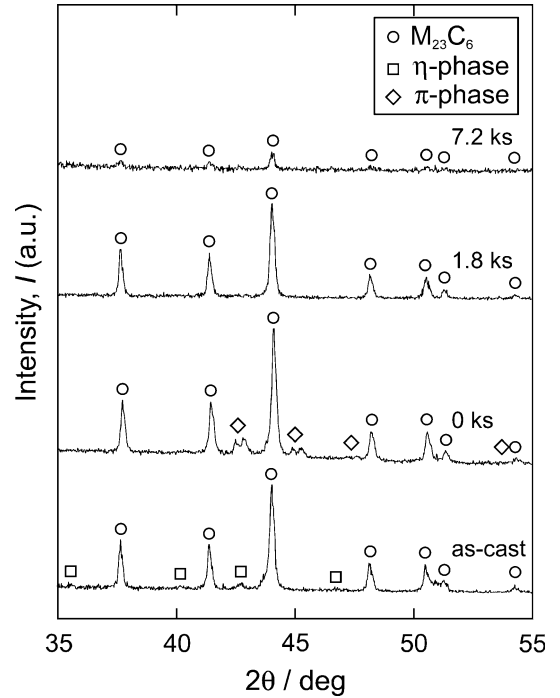


Fig. 12—Variation in the precipitates in the C35 alloy with holding time for heat treatment at 1548 K.

alloys with a carbon content of up to 0.28 mass pct and containing additional Si, Mn, and Ni after heat treatment at 1483 K for 230.4 ks.<sup>[11]</sup> These findings can be

explained by our results shown in Figure 7. Although the alloying elements such as Si, Mn, Ni, and N in Co-Cr-Mo-C alloys may affect the carbide dissolution behavior, an understanding of the complete precipitate

dissolution conditions in Co-Co-Mo-C alloys is essential not only for the heat treatment of castings but also for the thermomechanical treatment of wrought products in Co-Cr-Mo alloys.

From the results summarized in Figure 17, the main phase observed in the C15, C25, and C35 alloys during solution treatment was the  $M_{23}C_6$  type carbide. In addition, a  $\pi$  phase was detected in the as-cast C15 alloy and in the C15, C25, and C35 alloys after heat treatment at high temperature for a short holding time. Because complete precipitate dissolution was finally observed in all the alloys after heat treatment, the stable phase of the present alloy composition in the temperature range between 1473 and 1548 K is considered to be the  $\gamma$  phase. However, the nonuniformity in the as-cast alloys caused by segregation of Cr, Mo, and C during solidification may lead to the local formation of the  $\pi$  phase in the initial stage of heat treatment. Then, the  $\pi$  phase dissolves in the  $\gamma$  matrix when the alloy is homogenized. The  $\pi$  phase can be detected after a short heat treatment at higher temperatures such as 1523 or 1548 K and in the as-cast C15 alloy after cooling in the copper mold at a high cooling rate. Therefore, it can be concluded that the  $\pi$  phase was formed at high temperatures when the local

nonuniformity in composition was retained in the alloys, and the  $\pi$  phase is not a thermodynamically stable phase. To the best of the present authors' knowledge, the formation of the  $\pi$  phase in F75 Co-Cr-Mo alloys has not yet been reported. The presence of the  $\pi$  phase has to be considered in the microstructural control of Co-Cr-Mo-C alloys in practical applications such as the head of artificial hip joints.

A starlike carbide was observed after heat treatment at high temperatures such as 1548 K. Clemow and Daniell reported the starlike carbide in their specimen

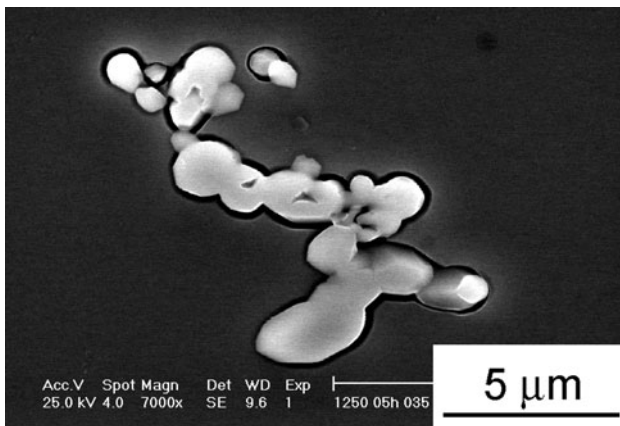


Fig. 13—SEM image of blocky-dense  $M_{23}C_6$  type carbide formed in the C35 alloy heat treated at 1523 K for 1.8 ks.

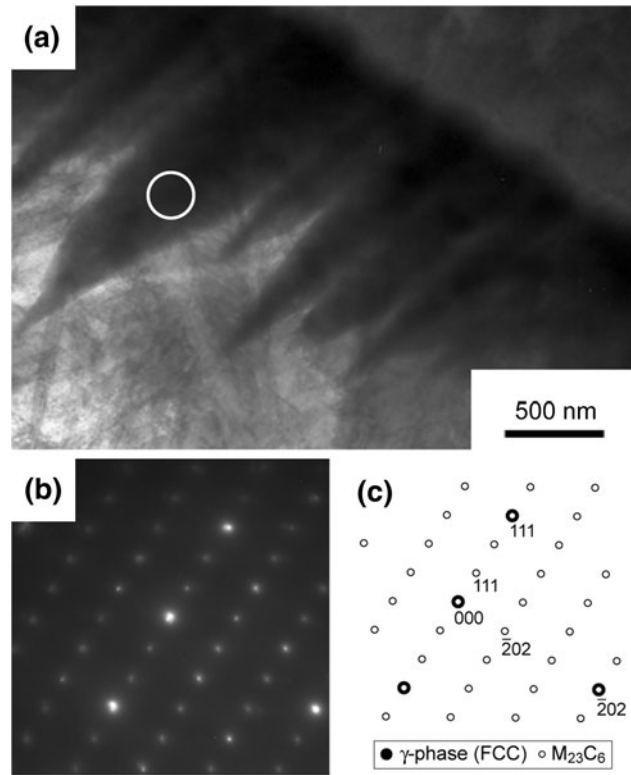


Fig. 15—TEM analysis of starlike precipitate with stripe pattern formed in C35 alloy that was heat treated at 1548 K for 0 ks. Beam direction along  $[1\bar{2}1]$ . (a) Bright field image, (b) associated diffraction pattern, and (c) schematic diagram identifying reflections in (b).

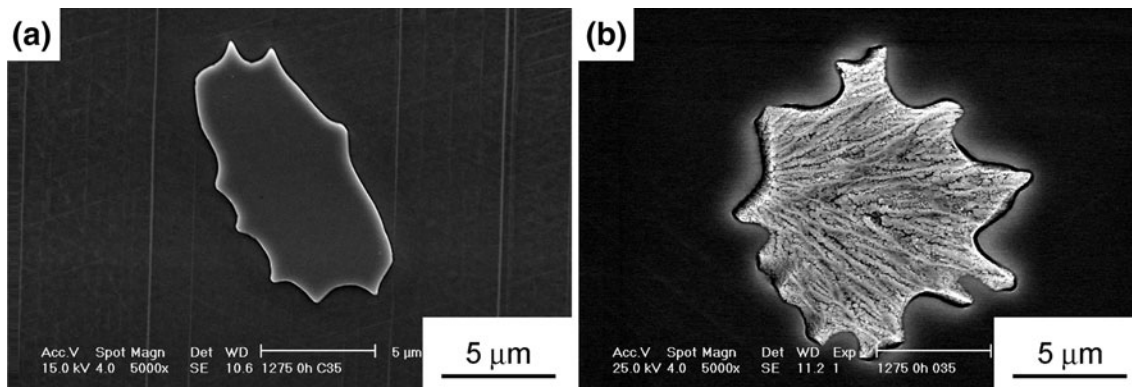


Fig. 14—SEM images of starlike precipitates formed in C35 alloy heat treated at 1548 K for 0 ks: (a) a starlike shape with no stripe pattern and (b) a starlike shape with stripe pattern.



alloy after heat treatment at 1503, 1523, and 1543 K.<sup>[11]</sup> In addition, they mentioned that this distinctive starlike shape was attributable to incipient melting around the

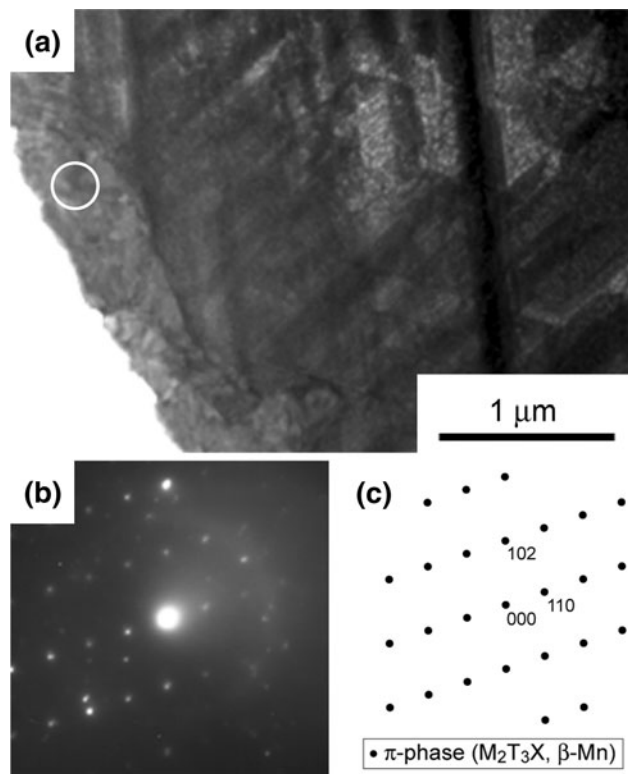


Fig. 16—TEM analysis of starlike precipitate with no stripe pattern formed in C35 alloy that was heat treated at 1548 K for 0 ks. Beam direction along [221]. (a) Bright field image, (b) associated diffraction pattern, and (c) schematic diagram identifying reflections in (b).

edges of the  $M_6C$  type carbide particles.<sup>[11]</sup> In this study, the  $M_6C$  type carbide could not be observed when starlike precipitates were found. However, the formation mechanism of starlike precipitates was likely to be related to the partial melting at the interface of the precipitate and the matrix, as suggested by Clemow and Daniell. The partial melting induced by the nonuniformity in composition might also be a factor in the formation of the  $\pi$  phase at high temperatures. Two types of starlike carbides could be observed in this study. One was a starlike carbide that had a stripe pattern; the other was a starlike-dense precipitate that did not have a stripe pattern. TEM analysis revealed that this stripe pattern consisted of the  $M_{23}C_6$  type carbide and  $\gamma$  phase. In this study, a blocky, not starlike, precipitate with stripe pattern, which consisted of the  $M_{23}C_6$  type carbide and  $\gamma$  phase, was also observed in as-cast alloys, and its amount increased with the carbon content. The precipitate with the stripe pattern observed in the as-cast and heat-treated alloys may have formed by the following reaction: liquid to  $M_{23}C_6$  type carbide and  $\gamma$  phase or  $\pi$  phase to  $M_{23}C_6$  type carbide and  $\gamma$  phase during heat treatment or during cooling processes such as casting and quenching.

## V. CONCLUSIONS

Precipitates in biomedical Co-Cr-Mo alloys with different carbon contents (0.12, 0.15, 0.25, and 0.35 mass pct) before and after heat treatment in the temperature range between 1473 and 1548 K for 0 to 43.2 ks were investigated. The following results were obtained.

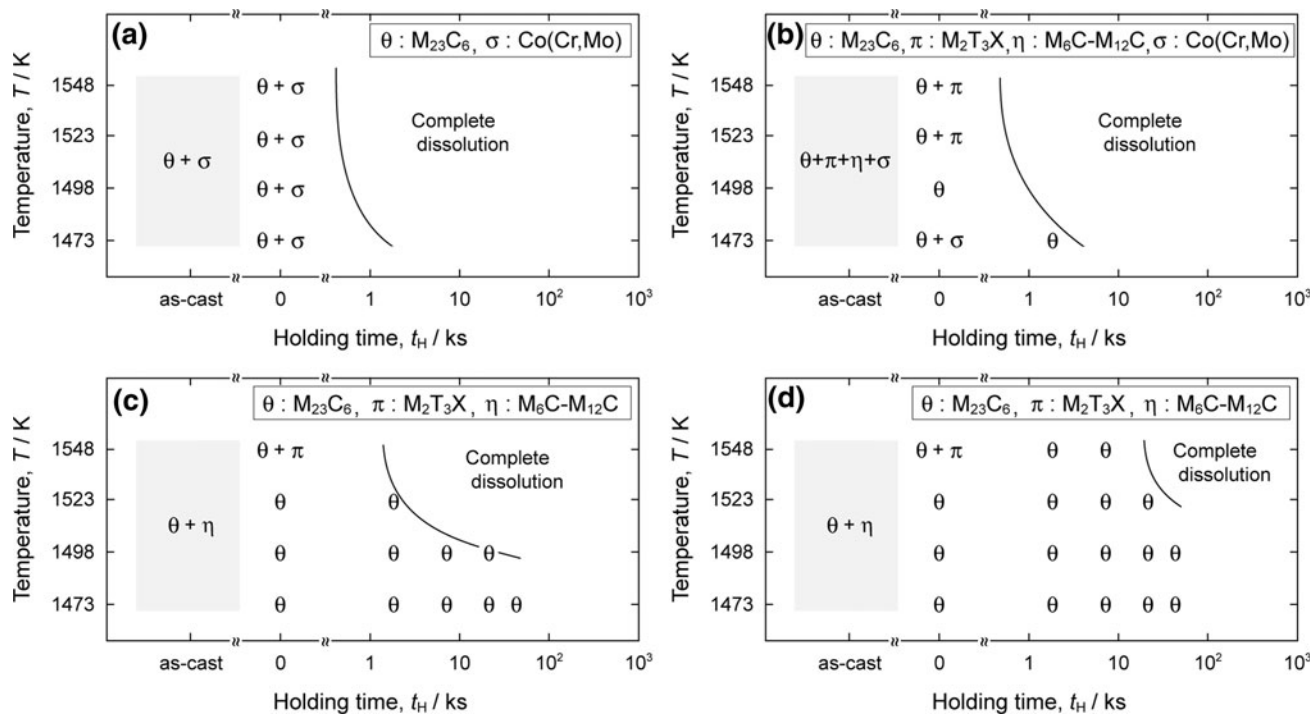


Fig. 17—Types of precipitates formed in the (a) C12, (b) C15, (c) C25, and (d) C35 alloys during solution treatment.

1. The precipitate detected in the as-cast alloys depended on the carbon content of the alloys. An  $M_{23}C_6$  type carbide and an intermetallic  $\sigma$  phase (Co(Cr,Mo)) were observed in the as-cast C12 alloy. An  $M_{23}C_6$  type carbide, an  $\eta$  phase ( $M_6C$ - $M_{12}C$  type carbide), a  $\sigma$  phase, and a  $\pi$  phase ( $M_2T_3X$  type carbide with a  $\beta$ -manganese structure) were detected in the C15 alloy. An  $M_{23}C_6$  type carbide and an  $\eta$  phase were detected in the C25 and C35 alloys.
2. Complete precipitate dissolution could be achieved in Co-Cr-Mo alloys with various carbon contents of up to 0.35 mass pct.
3. Under incomplete precipitate dissolution conditions, the  $M_{23}C_6$  type carbide and  $\sigma$  phase were observed in the C12 alloy, and the  $M_{23}C_6$  type carbide and  $\pi$  phase were observed in the C15, C25, and C35 alloys. The  $\pi$  phase was detected in alloys that were heat treated at high temperatures such as 1548 K for a short holding time of less than 1.8 ks. It was the first time that the  $\pi$  phase was detected in F75 Co-Cr-Mo alloys.
4. The morphology of precipitates formed in Co-Cr-Mo-C alloys depended on the heat-treatment temperature. The blocky-dense  $M_{23}C_6$  type carbide was detected at lower temperatures such as 1473 or 1493 K. At higher temperatures such as 1548 K, starlike precipitates were observed in the alloys. The starlike precipitate with a stripe pattern consisted of the  $M_{23}C_6$  type carbide and  $\gamma$  phase. In contrast, the starlike precipitate with no stripe pattern (starlike-dense precipitate) was the  $\pi$  phase.

#### ACKNOWLEDGMENTS

The authors thank Professor Hara and Mr. Soma, Tohoku University, for their useful suggestions on electrolytic extraction, and Dr. Kobayashi for his TEM works. The authors thank the Yoneda Advanced Casting Co., Ltd., for supplying the Co-Cr-Mo alloy ingots used in this study. This work was supported, in part, by the Global COE Program "Materials Integration, Tohoku University," MEXT, Japan.

#### REFERENCES

1. M. Niinomi: *Metall. Mater. Trans. A*, 2002, vol. 33A, pp. 477–86.
2. M. Niinomi, T. Hanawa, and T. Narushima: *JOM*, 2005, vol. 57, pp. 18–24.
3. S.H. Lee, E. Takahashi, N. Nomura, and A. Chiba: *Mater. Trans.*, 2006, vol. 47, pp. 287–90.
4. S.H. Lee, N. Nomura, and A. Chiba: *Mater. Trans.*, 2008, vol. 49, pp. 260–64.
5. P.C. Noble: *Met. Forum*, 1983, vol. 6, pp. 59–80.
6. L.J. Peterson, R.V. McKinney, Jr., B.M. Pennel, J.J. Klawitter, and A.M. Weinstein: *J. Dent. Res.*, 1980, vol. 59, pp. 99–108.
7. F.R. Morral: *J. Mater.*, 1966, vol. 1, pp. 384–412.
8. M. Caudillo, M. Herrera-Trejo, M.R. Castro, E. Ramírez, C.R. González, and J.I. Juárez: *J. Biomed. Mater. Res.*, 2002, vol. 59, pp. 378–85.
9. H.S. Dobbs and J.L.M. Robertson: *J. Mater. Sci.*, 1983, vol. 18, pp. 391–401.
10. M. Herrera, A. Espinoza, J. Méndez, M. Castro, J. López, and J. Rendón: *J. Mater. Sci.*, 2005, vol. 16, pp. 607–11.
11. A.J.T. Clemow and B.L. Daniell: *J. Biomed. Mater. Res.*, 1979, vol. 13, pp. 265–79.
12. J.W. Weeton and R.A. Signorelli: *Trans. Am. Soc. Met.*, 1955, vol. 47, pp. 815–52.
13. H. Mancha, E. Carranza, J.I. Escalante, G. Mendoza, M. Méndez, F. Cepeda, and E. Valdés: *Metall. Mater. Trans. A*, 2001, vol. 32A, pp. 979–84.
14. C. Montero-Ocampo, M. Talavera, and H. Lopez: *Metall. Mater. Trans. A*, 1999, vol. 30A, pp. 611–20.
15. T. Kilner, R.M. Pilliar, G.C. Weatherly, and C. Allibert: *J. Biomed. Mater. Res.*, 1982, vol. 16, pp. 63–79.
16. F.J. Clauss, F.B. Garrett, and J.W. Weeton: *NACA*, 1955, TN 3512.
17. R.N.J. Taylor and R.B. Waterhouse: *J. Mater. Sci.*, 1983, vol. 18, pp. 3265–80.
18. L.E. Ramirez, M. Castro, M. Méndez, J. Lacaze, M. Herrera, and G. Lesoult: *Scripta Mater.*, 2002, vol. 47, pp. 811–16.
19. J. Jeciejewicz: *J. Less-Common Met.*, 1964, vol. 7, pp. 318–20.
20. A.C. Fraker and H.H. Stadelmaier: *Trans. TMS-AIME*, 1969, vol. 245, pp. 847–50.
21. D.S. Janisch, M. Garel, A. Eder, W. Lengauer, K. Dreyer, and H. van den Berg: *Int. J. Refract. Met. Hard. Mat.*, 2008, vol. 26, pp. 179–89.
22. J.M. Guilemany, J.M. de Paco, J. Nutting, and J.R. Miguel: *Metall. Mater. Trans. A*, 1999, vol. 30A, pp. 1913–21.
23. JCPDS card 26-0428.
24. M. Kikuchi, S. Wakita, and R. Tanaka: *Trans. ISIJ*, 1973, vol. 13, pp. 226–28.
25. W. Jeitschko, H. Nowotny, and F. Benesovsky: *Mh. Chem.*, 1963, vol. 94, pp. 247–51.